Geomorphology 134 (2011) 260–268

Contents lists available at ScienceDirect

Geomorphology

journal homepage: www.elsevier.com/locate/geomorph

Object-based gully feature extraction using high spatial resolution imagery

Rajesh B.V. Shruthi *, Norman Kerle, Victor Jetten

Department of Earth Systems Analysis, Faculty of Geo-Information Science and Earth Observation (ITC), University of Twente, Netherlands

ARTICLE INFO

Article history:
Received 22 September 2010
Received in revised form 17 June 2011
Accepted 4 July 2011
Available online 21 July 2011

Keywords:
Gully erosion
Object-based image analysis
Land degradation
High spatial resolution imagery

ABSTRACT

Gully erosion is responsible for a substantial amount of soil loss and is generally considered an indicator of desertification. Hence, mapping these gully features provides essential information needed on sediment production, identification of vulnerable areas for gully formation, land degradation, and environmental and socio-economical effects. This paper investigates the use of object-oriented image analysis (OOA) to extract gully erosion features from satellite imagery, using a combination of topographic, spectral, shape (geometric) and contextual information obtained from IKONOS and GEOEYE-1 data. A rule-set was developed and tested for a semi-arid to sub-humid region in Morocco. The percentage of gully system area indicated negligible overestimations between the reference area and the OOA area in two sub-watersheds (0.03% and 1.77%). We also observed that finer gully-related edges within the complex gully systems were better identified semi-automatically than was possible by manual digitization, suggesting higher detection accuracy. OOA-based gully mapping is quicker and more objective than traditional methods, and is thus better suited to provide essential information for land managers to support their decision making processes, and for the erosion research community.

1. Introduction

Erosion by surface runoff has been receiving substantial attention from researchers, conservationists and policy makers. It comprises sheet or inter-rill, rill and gully erosion. Amongst these forms of soil removal, gully erosion in both ephemeral and permanent gullies is responsible for a substantial amount of soil loss, and is generally considered an indicator of desertification (UNEP, 1994). Fig. 1 illustrates a typical gully formation situation, with incisions frequently cutting through different soil horizons, and their form and shape being guided by the hydrological and mechanical properties of these soil layers. A second commonly occurring gully formation process is the backward extension of a gully in the hillslope, which occurs as a combination of water incision and small mass movement on the sides and head of a gully. Extensive reviews on the initiation, controlling factors and impacts of gullying have been provided by Poesen et al. (2003) and Valentin et al. (2005). Poesen et al. (2006) and Vrieling et al. (2007) also identified that most research has focused on sheet (inter-rill) and rill erosion, and that little is known about gully erosion and its importance at large spatial scales. One of the reasons is that gullies, once formed, can remain unaltered for extended periods of time, especially in semi-arid climates. Although they are evidence of severe land degradation, their dimensions may not be easily related to current rainfall (Seeger et al., 2009) and surface runoff (Marzolff and Ries, 2007). Moreover, the timeframe at which they formed and changed is often unclear.

Sustainable land management fundamentally requires knowledge of the landscape and its processes, for which an efficient way of understanding, surveying and monitoring is needed. Given that gullies are one of the main drivers for soil loss in the landscape system, there is an imperative need for detailed monitoring and better prediction of gully locations. This study focuses on rill/ephemeral and permanent gully erosion. The gully features investigated are discontinuous, and much narrower (<10 m) than gullies on a river bank (alluvial gullies) with widths of 20 to 140 m (Brooks et al., 2009; Perroy et al., 2010). This constitutes a real challenge for the semi-automatic detection of gullies, because of not only the size, shape and distribution of gullies but also the presence of various land cover, land use, shadow and illumination. This study attempts to address the two existing problems: 1) mapping gully systems through field work and manual image digitization are difficult and time consuming, and 2) there is a lack of a generic algorithm to identify gullies from images.

Mapping gullies and erosional activity is crucial for monitoring erosion and studying its impacts including sediment production, land degradation, and other socio-economical influences. Field-based methods were used in the past until aerial photos and later satellite imagery became more readily available. Remote sensing-based mapping is the only practical approach for mapping gully features over large areas, given the variability in gully size, shape and occurrence (Knight et al., 2007), as well as the dynamic nature of gully-affected landscapes. A review of different methods used to map and monitor gully erosion features is given below. It has been recognized that accurate identification of gullies is not possible without additional data or expert knowledge (Bocco and Valenzuela, 1993). In addition auxiliary information, such as geometric properties (shape, dimension, orientation and texture) and the

* Corresponding author. Tel.: +31 53 4874504; fax: +31 53 4874336.
E-mail address: shruthi@itc.nl (R.B.V. Shruthi).

0169-555X/$ – see front matter © 2011 Elsevier B.V. All rights reserved.
doi:10.1016/j.geomorph.2011.07.003

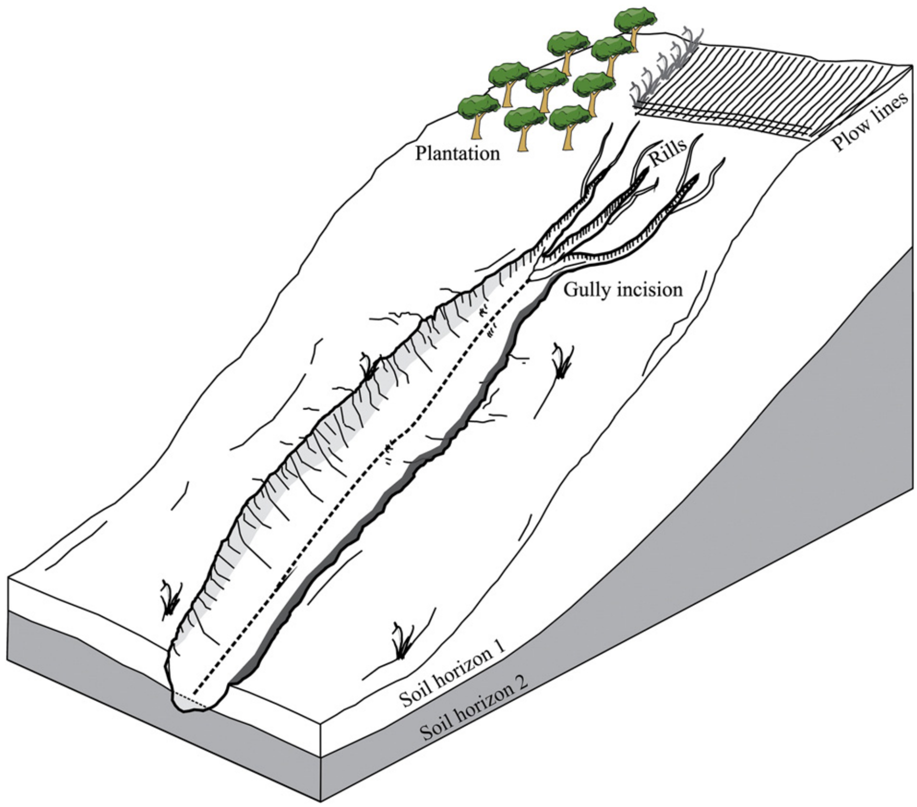

Fig. 1. Schematic illustration of a gully formed by the deepening of rills. Gullies develop if rills do not disappear because of tillage.

spatial relationship with surrounding features, allows an approach fundamentally similar to the cognitive approach used in visual image assessment, but in a controlled and reproducible quantitative manner. This makes it possible to treat erosion features as spatial objects that can be characterized based not only on their geometric properties, but also on their spatial relationship with surrounding features. The potential of object-oriented image analysis (OOA, also referred to as object-based image analysis - OBIA) to map gully erosion features from high spatial resolution optical imagery has rarely been explored. The objectives of this study are to: 1) examine the potential of OOA to map complex gully erosion features using high spatial resolution imagery (HRI); 2) establish the topographical and image thresholds (spectral and textural) for a given area and develop a generic method for semi-automatic gully detection and extent mapping; and 3) assess the accuracy of the results by comparing them with the manually digitized gully system.

2. Previous works on mapping and monitoring gullies using remote sensing

Contributions of remote sensing to soil erosion research based on aerial photos and image interpretation techniques date back to the 1940s (Smith, 1943). Gully erosion assessment by aerial photo interpretation and photogrammetric techniques continued largely unchanged for decades (Langran, 1983; Stromquist et al., 1985). These studies were limited to visual image interpretation of photos, which are generally collected for smaller regions of interest, not frequently acquired, typically housed in archives that are not readily cataloged and accessible, and have no multi-spectral information. With the launch of Landsat-1 in 1972, satellite imagery became available to the scientific community. The increasing availability of spaceborne data with suitable spatial and spectral information (400–1000 nm), swath width ranging from 185 to 950 km and frequent revisits, allows the detection of erratic instances of land degradation, gradually rendering airborne data less relevant. Visual analysis, a logical follow-up to aerial photo interpretation, was successfully used to delineate gully features using Landsat imagery (Singh, 1977). Until recently pixel-based image analysis, using only the surface reflectance values, has been the main method to extract gullies (Bocco et al., 1991; Metternicht and Zinck, 1998). Various pixel based classification methods (Lillesand et al., 2008) can be employed for thematic mapping and quantitative analysis of eroded areas. However, the selection of adequate training pixels (a key element for a successful classification) requires an in-depth knowledge of the study area and careful analysis of the separability of spectral signatures (Laliberte and Rango, 2009). In addition, spectral heterogeneity of the environment is affected by variability in moisture, organic matter, and mineral content, and also shadow and atmospheric influences add to a given texture. This strongly affects the performance of multispectral image classifications. Furthermore, the spatial resolutions of the first generation's Earth observation sensors and platforms, such as those onboard of Landsat, SPOT, ASTER, IRS and ENVISAT, were only sufficient to identify large to medium sized gullies (Vrieling and Rodrigues, 2004). Technical developments in spaceborne remote sensing, such as higher spatial and temporal resolution, the increased availability of rational polynomial coefficient-based digital surface models (DSMs) that only requires minimal ground data (Martha et al., 2010a), and development and extension of digital imaging technology and GIS, have created new possibilities for research in gully erosion. However, their potential for erosion feature mapping remains largely unassessed. Studies that used more advanced methods, such as spectral linear unmixing (De Asis et al., 2008) or a multitemporal approach (Vrieling et al., 2007), yet were limited to the pixel level, inevitably faced challenges from spectrally similar false positives. Working with HRI implies a substantial increase in the number of pixels and information to be handled during the analysis, and even larger spectral ambiguity. This means that spectral variability associated with gully features, such as the presence of vegetation, or shadow- or moisture-related brightness differences, cannot be effectively captured with a method purely based on spectral information. With growing availability of HRI, a shift away from traditional pixel-based methods has been necessary. The analysis of objects or features, as opposed to individual pixels, is more appropriate to address the aforementioned heterogeneity, and more suitable for knowledge-driven analysis akin to visual image interpretation. A comprehensive review on the development and applications of OOA can be found in Blaschke (2010). Some gully mapping studies using OOA have already been carried out. Knight et al. (2007) used ASTER imagery to map alluvial gullies associated with large tropical rivers, while Eustace et al. (2009) used high-resolution LiDAR data to successfully map gully extent and density using OOA. The characteristics of neither dataset are comparable to what is contained in high resolution optical images, hence the studies offer limited guidance for the work with modern optical satellite data. The work by Knight et al. (2007), who only obtained accuracies for the gully class of approximately 50%, also showed that an object-based approach does not automatically lead to superior results. OOA has shown promising results in related application areas where the integration of multi-type auxiliary information has aided the analysis, such as landslide detection (Martha et al., 2010b), or field boundary extraction (Chen et al., 2009; Tansey et al., 2009). Insights from these studies, as well as recent work that has made OOA more objective and less based on trial-and-error (Martha et al., in press; Stumpf and Kerle, in press) are reflected in our work to improve gully identification and mapping with HRI.

3. Study area

The processing approach was developed and tested for two areas covering approximately 0.99 km^2 and 0.84 km^2, respectively, in the Sehoul commune region, Morocco (Fig. 2). Both are part of the lower central plateau Atlantic Meseta. The climate in this region ranges between sub-humid and semi-arid, with a mean annual rainfall of 350 mm over a 32 year period (1970–2002), collected at the Rabat/Sale meteorological station about 22 km away from the study area (DESIRE, 2010). Most of the region consists of rolling-hill topography. Land use consists of cork oak forests, agriculture (rain-fed wheat, barley and maize), horticulture (mint, beans, and courgette) and orchards, with some fields being irrigated (submersion and drip). Eucalyptus plantations for timber and fire wood can also be found in some parts of the region. The major reason for extensive land degradation has been accounted to excessive grazing by the livestock (van Dijck et al., 2006).

Due to the increasing population pressure (both human and livestock) the region has been undergoing major land use changes, such as the trend towards replacing natural forests with exotic species (eucalyptus), and intensification of traditional land uses with corresponding reduction of fallow periods and overgrazing in natural areas, despite the weak production of vegetation and readily erodible soils. The reduction of organic matter and vegetation cover also results in soil compaction and higher overland flow generation in the overgrazed areas, increasing chances of gully incision at flow concentration zones. Extensive gully systems are found on abandoned lands and in overgrazed areas at the sloping edge of the Marmora plateau (DESIRE, 2010). Fig. 3 illustrates different forms of gully occurrence in the study area.

4. Data and methods

Orthorectified IKONOS data acquired on 31 December 2005 (blue, green, red and NIR of 4 m resolution, and PAN data of 1 m resolution; P-B-G-R-NIR) were used for extracting the spectral and spatial information. Stereoscopic GEOEYE-1 data (PAN-0.5 m resolution) acquired on 1 September 2009 were used to create a DSM. The subsequent sections provide details of the methodology adopted (Fig. 4).

4.1. DSM generation

The photogrammetric software SAT-PP, developed by ETH Zurich (Zhang and Gruen, 2006), was used to generate a 1 m DSM (representation of the earth surface along with the above ground features such as vegetation, and manmade features) from the GEOEYE-1 stereo-pair, together with the rational polynomial coefficients (RPCs). Nine ground control points obtained from a differential GPS (DGPS) survey were used to improve the orientation result of the RPC model. A vertical root mean square error (RMSE) of 0.37 m was achieved. Further, a digital terrain model representing only the earth surface excluding the above ground features (DTM), essential for quantifying topographic parameters, was derived from the DSM. The accuracy of the parameters mainly depends on the accuracy of the DTM (Dragut and Blaschkeb, 2006). Hence, the following corrections were made using Leica Photogrammetric Suite (LPS). Local artifacts in the DSM, e.g. those resulted from scattered vegetation patches and buildings, were

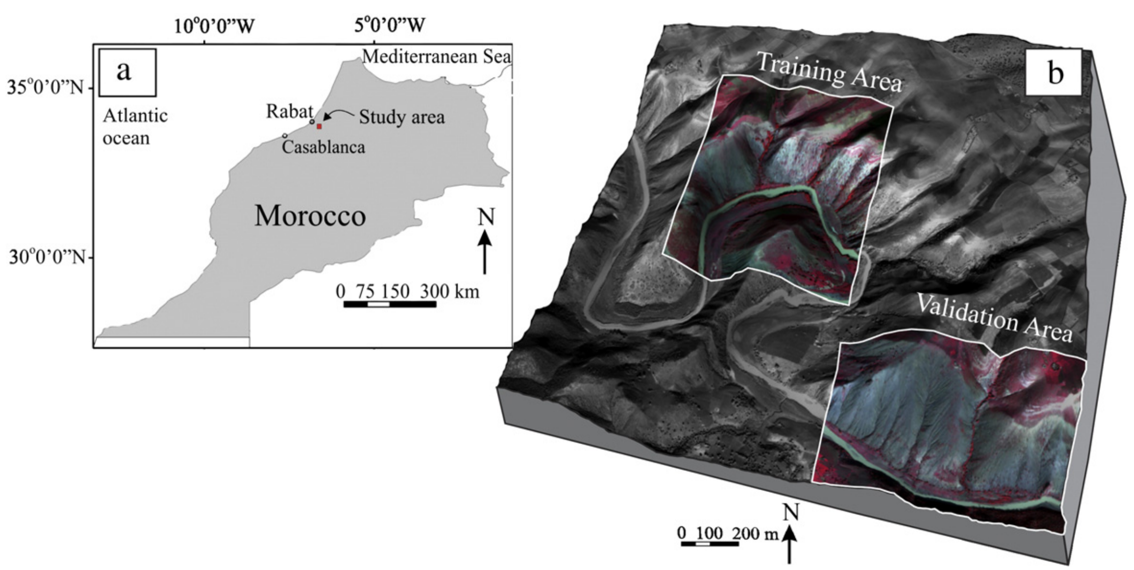

Fig. 2. The study area. (a) Location. (b) PAN data overlaid on the DTM, and showing the training and validation areas as false color composites.

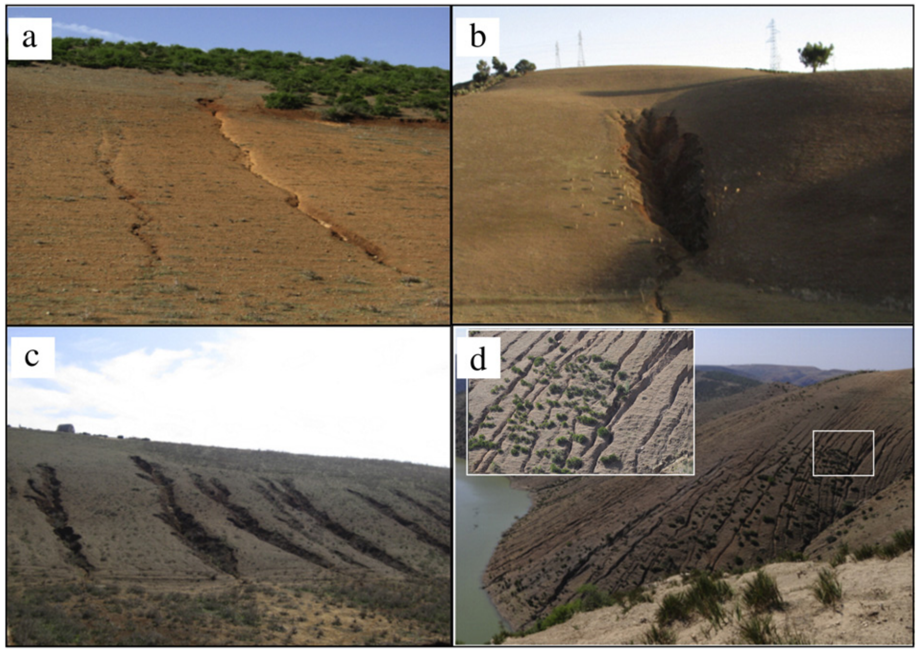

Fig. 3. Diversity in gullies in the Sehoul commune region. (a) Rill and ephemeral gully. (b) Simple isolated gully. (c) Simple continuous gully system. (d) Complex discontinuous gully system.

removed to avoid large errors in DTM derivatives (Martha et al., 2010a). Particular areas such as streams, rivers, and deep gullies, where the vertex or elevation values appeared to be erroneous, were also corrected manually using 3D break-lines. Finally, the DTM was hydrologically corrected using SAGA (Böhner et al., 2006) to allow extraction of derivatives such as slope, flow direction, specific catchment area (*SCA*) and sub-watersheds. These derivatives, along with the DTM, were used as input layers for OOA.

4.2. Gully feature extraction

Feature extraction was carried out in eCognition Developer 8 that uses an object-oriented approach for semi-automated image analysis. Baatz and Schäpe (2000) give a detailed description of the concept and its implementation in eCognition.

4.2.1. Texture measure based on flow direction

Various studies have demonstrated that the use of texture metrics, e.g. derived from the Gray Level Co-occurrence Matrix (GLCMs) (Haralick et al., 1973), can significantly enhance the efficiency of image classification algorithms (Laliberte and Rango, 2009). Direction is significant when distinguishing gullies from non-gully features. Gullies

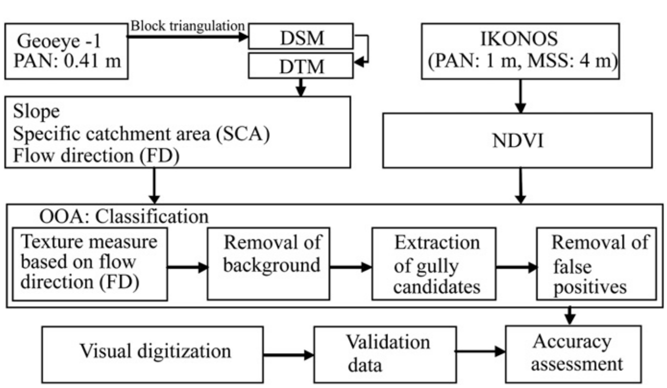

Fig. 4. Overview of the method of gully feature extraction.

are generally directed along the slope following the flow direction, while features such as freshly ploughed land, which has spectral and textural properties similar to gullied area, usually run slope parallel (at least within the study area where tillage operations are non-mechanical). To quantify such features and distinguish them from gullies, a set of rotation-variant GLCMs metrics ($GLCM_{CON}$ for contrast and $GLCM_{COR}$ for correlation) was calculated based on the flow direction. The first step was to resample the original DTM to 10 m (this step degrades the quality of flow direction; however, it will still follow the direction specific to the aspect). This was done in order to create an artificial flow direction boundary that could include a sufficient number of PAN pixels to identify directionality in the texture. Then flow direction (*FD*) was calculated (Greenlee, 1987) and categorized into four main classes: N–S (0°), NE–SW (45°), E–W (90°) and NW–SE (135°). Subsequently, within each flow direction segment the normalized GLCMs of the IKONOS PAN data (10×10 pixels) were calculated in the direction of flow ($P_{i,j(FD)}$) and perpendicular to the flow ($P_{i,j(FD-90°)}$). In particular the quotients of $GLCM_{CON\perp}$ (Eq. 2) and $GLCM_{COR\perp}$ (Eq. 5) perpendicular to flow direction were used to highlight areas.

$$P_{i,j} = \frac{V_{i,j}}{\sum_{i,j=0}^{N-1} V_{ij}} \tag{1}$$

$$GLCM_{CON\perp} = \frac{\sum_{i,j=0}^{N-1} P_{i,j(FD)}(i-j)^2}{\sum_{i,j=0}^{N-1} P_{i,j(FD-90^\circ)}(i-j)^2} \tag{2}$$

$$\mu_{i,j} = \frac{\sum_{i,j=0}^{N-1} P_{i,j(FD)}}{N^2} \tag{3}$$

$$\sigma_{i,j} = \sqrt{\sum_{i,j=0}^{N-1} P_{i,j(FD)}\left(i,j-\mu_{i,j}\right)} \tag{4}$$

$$GLCM_{COR\perp} = \frac{\sum_{i,j=0}^{N-1} P_{i,j(FD)} \frac{(i-\mu_i)(j-\mu_j)}{\sqrt{(\sigma_i^2)(\sigma_j^2)}}}{\sum_{i,j=0}^{N-1} P_{i,j(FD-90^\circ)} \frac{(i-\mu_i)(j-\mu_i)}{\sqrt{(\sigma_i^2)(\sigma_j^2)}}} \tag{5}$$

where, i is the row number, j is the column number, N is the number of rows or columns, $V_{i,j}$ is the value in the cell i,j of the matrix, $P_{i,j}$ is the normalized value in the cell i,j, $\mu_{i,j}$ the mean of the texture, and $\sigma_{i,j}$ the std. deviation of the texture. Fig. 5 illustrates that grey values along a gully (downslope) are typically more correlated than in directions quasi-perpendicular to the slope. These layers were exported as image layers and used as additional input layers in the eCognition project, resampled to the highest resolution in the project, i.e. 1 m.

4.2.2. Removal of background or areas of non-interest

As discussed above, large amounts of information need to be handled to work with HRI results. Hence, it is beneficial to remove most of the segments of non-interest or background to achieve better efficiency and results. Most of the areas with relatively low *SCA*, areas that are flat to gentle slope and are textured predominantly perpendicular to the flow direction (quasi-linear features such as plough lines), as well as vegetation and shadow, were classified as background and excluded from further analysis. The optimal scale for segmentation, a critical step that strongly influences the subsequent analysis (Martha et al., in press), was estimated using the Estimation of Scale Parameter (ESP) developed by Dragut et al. (2010). First a multi-resolution segmentation, based on a homogeneity criterion composed of shape and compactness factors that determine the best neighbor to merge with a scale factor of 72, was applied on the DTM and slope to remove most of the segments that have relatively lower *SCA*, and areas with flat to gentle slope. Subsequently the unclassified area was further segmented using multiresolution on the P-B-G-R-NIR bands with a scale parameter of 92, also derived from ESP, to remove most of the other background areas. Segments that were not successfully classified as background in this step were later removed as false positives (Section 4.2.4).

4.2.3. Extraction of gully candidates

The segments that were left unclassified after the removal of background were further segmented by chessboard segmentation with object size 1, which divides the image or selected parts into equal squares of a given size, in this case to re-establish the original image components (pixel level). Then a contrast filter was applied on the PAN data, to enhance features in shadowed areas and dark boundaries. This was used to identify potential gully segments and later merged. In the second step a Lee-Sigma edge detection filter was applied on the PAN data to extract dark edges, i.e. sharp brightness transitions. This process detects object outlines, as well as boundaries between objects and the background in the image. This was used to extract gully systems within the potential candidates, including actual gullies but also a variety of false positives that were subsequently removed (Fig. 6).

4.2.4. Removal of false positives

The final step in gully feature extraction was the removal of false positives, i.e. other quasi-linear features that were miss-classified as gullies, and which include segments identified as a result of locally erroneous DSM derivatives, such as slope along vegetation boundaries that are modeled as small humps in the photogrammetrically derived elevation layer, cattle tracks, plough lines orthogonal to the slope, and small bright patches likely corresponding to rock outcrops.

4.2.5. Generation of reference data for accuracy assessment

While accuracy assessment is typically reduced to a mathematical problem based on comparison of analytical results and reference data, the intended use of the derived information also matters. This means that it is not so meaningful to match individual erosion elements in the system. This is because the production of complete reference data (e.g. by digitizing) is challenging, but also because of the partial limitations in its utilization from an information user's perspective. Because an extended gully system limits the utility of land, the extent of gullies is the most important parameter. We determined the percentage of gully system area in two different sub-watersheds, one consisting of simple and continuous (sw11) and the other complex and discontinuous (sw12) gully system, and examined the difference between reference and classified data. Reference data was generated by visual image interpretation and field observation. Polylines were digitized over individual gullies and then converted to a raster form, since direct matching of gully vectors resulting from the OOA analysis with digitized lines is too strongly affected by digitizing inaccuracies. Hence, instead of individual erosion lines, polygons showing a gully system were digitized by connecting the gully incision points identified in reference (A_{REF}) and classified (A_{OOA}) gully systems, using the convex hull approach (Melkman, 1987).

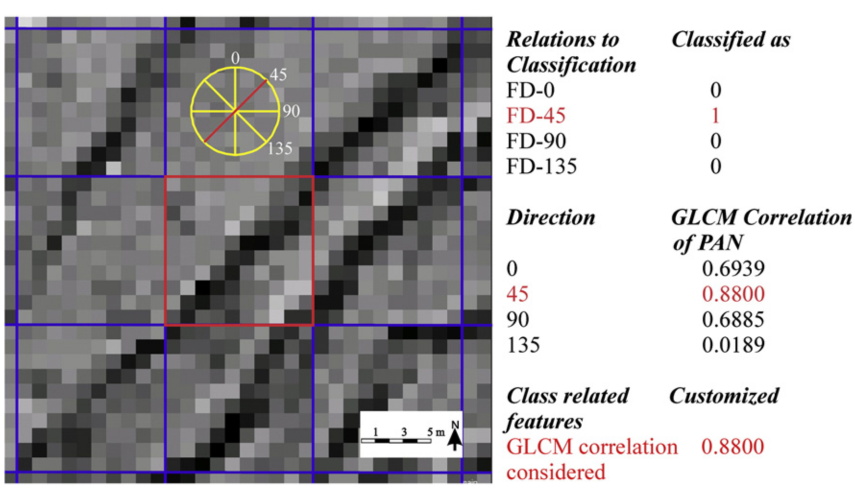

Fig. 5. Determining the texture value for a segment (GLCMs correlation along the flow direction). The yellow circle with four axes is flow direction at 0°, 45°, 90° and 135°. An example of assessing GLCM correlation of PAN for a segment with flow direction as 45°, identified in the red box (also indicated by the red axis in the circle).

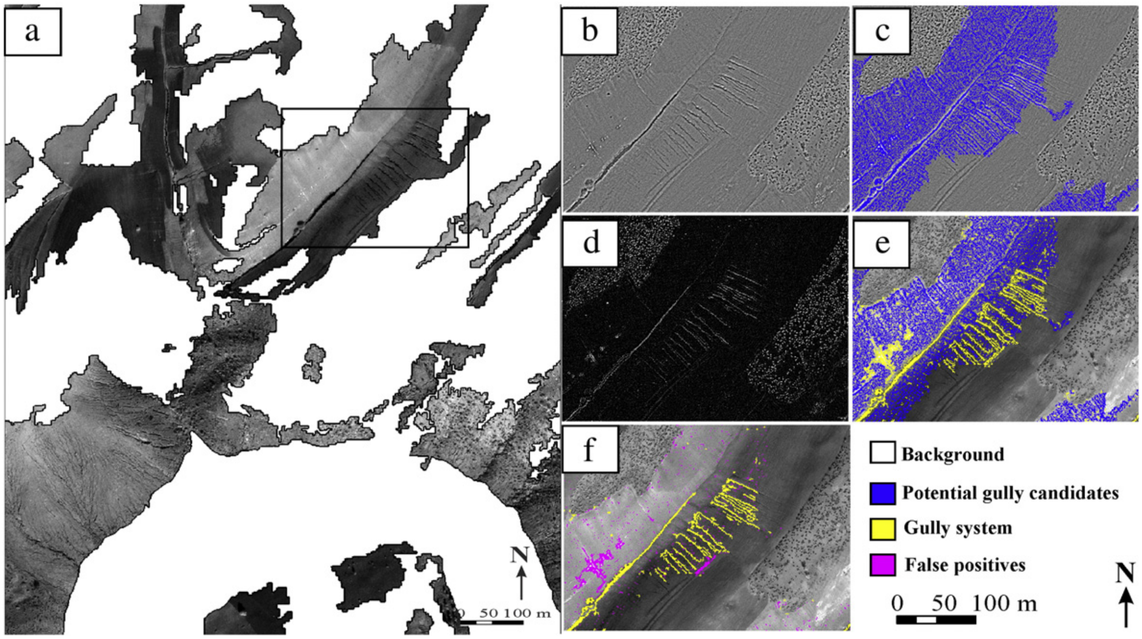

Fig. 6. Step of extracting gully erosion features using the OOA method. (a) Segments with background class for the test region. (b) Contrast filter on PAN data for the subset shown in black rectangle. (c) Potential gully candidates. (d) Sigma-Lee edge filter on the PAN image. (e) Gully system identified from potential candidates. (f) Gully system separated from false positives.

5. Results and discussion

As identified in the objectives, we examined the potential of OOA to map complex gully erosion features and established the topographical and image thresholds for a given area, to develop a generic method for semi-automatic gully detection to map the gully extent. Initial classification of all background classes eliminated areas of non-interest, thus improving the performance of classification processes by limiting subsequent steps to the unclassified region. Segments with $SCA \leq 40$ m^2 and areas with slope gradients < 3°, where surface runoff generation and accumulation are assumed to be insufficient for gully initiation, were removed. Later segments with $NDVI > 0.32$ were classified as vegetation, brightness < 170 as shadow, brightness > 330 for bright saturated areas that contain insufficient information for processing, and $GLCM_{COR\perp} < 1$ and $GLCM_{CON\perp} > 1.7$ for textured areas that are perpendicular to flow direction. Fig. 6 a illustrates a subset of the area with most of the background class.

In addition to the convention of using suitable topographic and vegetation thresholds, the use of contrast and edge filter information helped recognize potential gully candidates. Segments with contrast filter mean values < 0 were classified as potential gully candidates (Fig. 6 b,c). Later, segments with mean Lee-Sigma > 10 were classified as gullies, which include actual gullies, but also a variety of false positives that were subsequently removed (Fig. 6 d,e). A combination of different thresholds and geometric indicators was used to remove false positives (Fig. 6 f) as described in Table 1.

Table 1
Criteria for excluding false positives.

False positives	Criteria type	Description of criteria
Vegetation (shrubs, hedge rows crops from agricultural lands)	Spectral	Relatively higher *NDVI* Mean $NDVI \geq 0.25$
Shadow	Spectral	Maximum difference ≥ 0.6
Isolated objects with insufficient area	Geometric	Area ≤ 2
Bright patches	Spectral	Relatively higher *NIR* Mean $NIR \geq 410$

Fig. 7 illustrates the gully systems in the training area. Note how other linear features similar to gullies have been effectively eliminated (ellipses); while some false positives are still present (squares). In the test image an area of ca. 81,000 m^2 is affected by gully systems, i.e. ca. 8% of the total area.

The same rule-set, without parameter modification, was used to test the performance of gully identification in a different region within the same dataset. Fig. 8 illustrates the gully systems in the validation area. The total area affected by gullying was estimated at ca. 150,000 m^2, i.e. ca. 18% of the total area. It must be noted that the relatively low erosion level (8% and 18% of the total area in training and validation site respectively) may render the land around the gullies useless because of possible future erosion.

While a visual assessment of the results indicates realistic detection of gullies, feature extraction accuracy and uncertainties should be evaluated. The different gully systems in the two sub-watersheds, sw11 and sw12 (Fig. 9 a–d) show that the OOA analysis resulted in a slight overestimation of gully system area (A_{OOA}), compared to the reference area (A_{REF}), 85 m^2 for sw11 and 1529 m^2 for sw12, corresponding to 0.03% and 1.77% of the respective sub-watershed areas (Table 2). However, part of the apparent overestimation can be attributed to the problems with reference data preparation described in Section 4.2.5. In addition, increasing gully complexity led to more false positives and the gully system area in OOA. However, some increased false positives were acceptable, as they also ensure the transferability of the rule-set to other areas.

Uncertainties in this study can be assessed in terms of positional accuracy. Evaluation of this is important especially when heuristic generalization methods are applied. The DTM plays an important role in integrating the GIS and remote sensing data, especially in the orthorectification of the images, and the accuracy of the DTM used affects the accuracy of the final rectified image (Shi et al., 2005). A number of uncertainties relate to the spatial resolution and accuracy of the photogrammetric DTM used, and the derivatives calculated from it. This especially concerns local slope values that are highly sensitive to artifacts. Additional uncertainties were introduced by the images used in the study. The orthorectified IKONOS image used was not provided with the file of RPC (rational polynomial coefficients). In addition, no information was provided by the data vendor on the

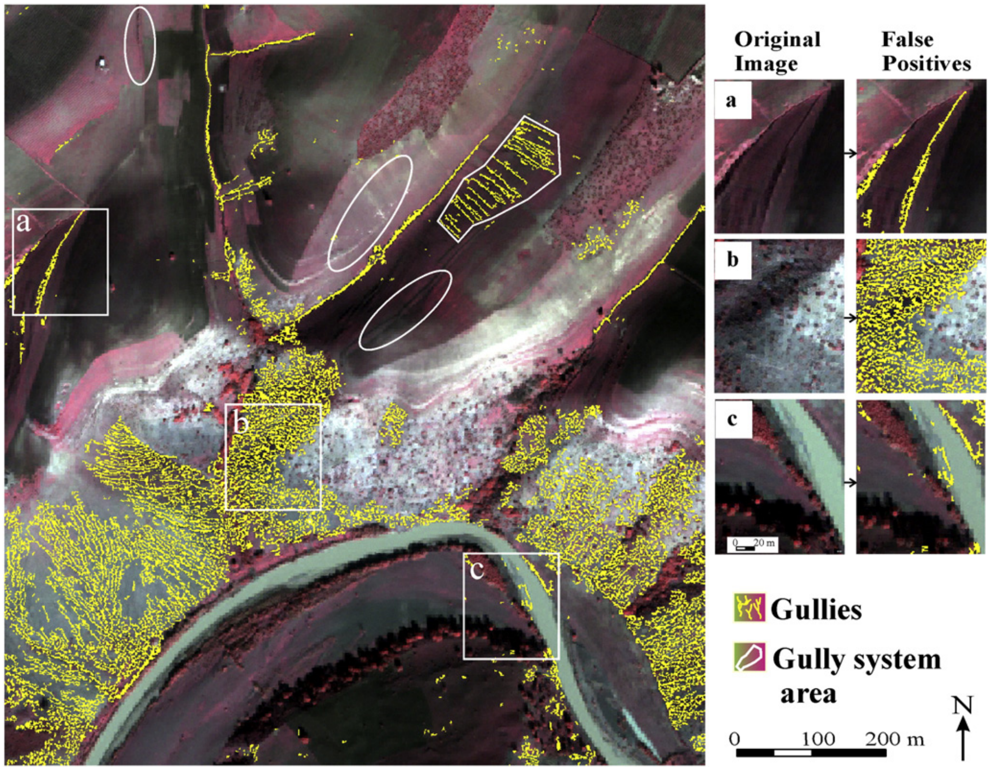

Fig. 7. Gully systems extracted by OOA in the training area, and linear features that appear gully-like have been effectively eliminated (ellipses), while some false positives are still present (squares); (a, b, and c) original image and the false positives for three of the instance identified in the squares.

topographic data used for the orthorectification of the image. We, therefore, performed an additional image-to-image registration with the flow accumulation image derived from our DSM, though some error may have propagated, leading to improper removal of background segments. Due to this we were unable to use some of the essential conditions such as flow accumulation, and curvature for developing the rule-set.

6. Conclusions

Accurate and comprehensive information of erosion features is of critical importance for farmers, land managers and scientists. To achieve this we firstly need to know gully location and extent, and our study introduces a method to provide this essential information. Our semi-automatic method is based on an algorithm or rule-set for

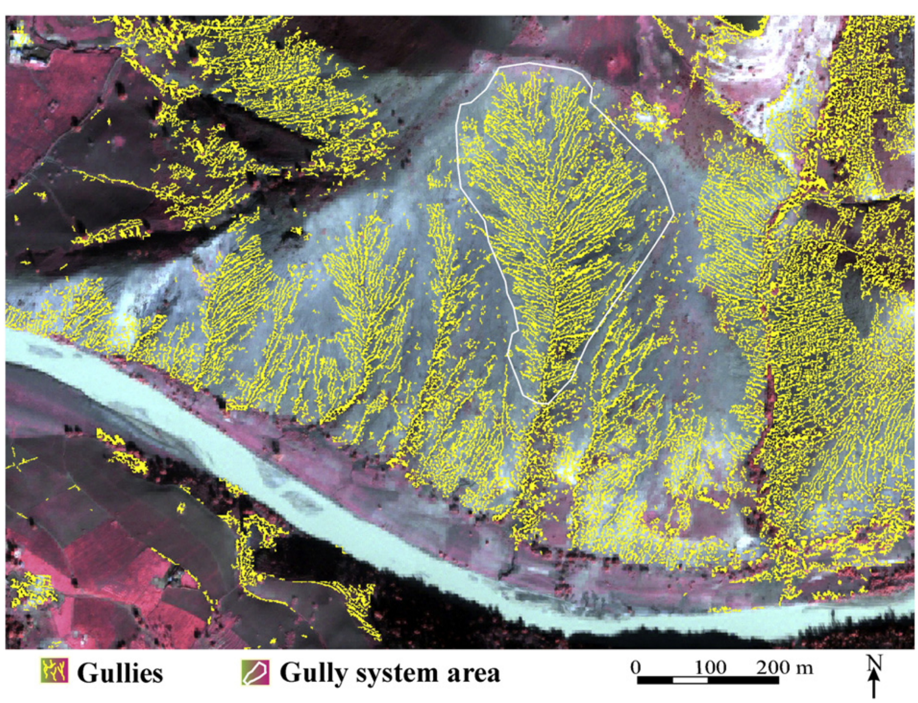

Fig. 8. Gully systems extracted by the rule-set developed in the validation area to test transferability of the rule-set.

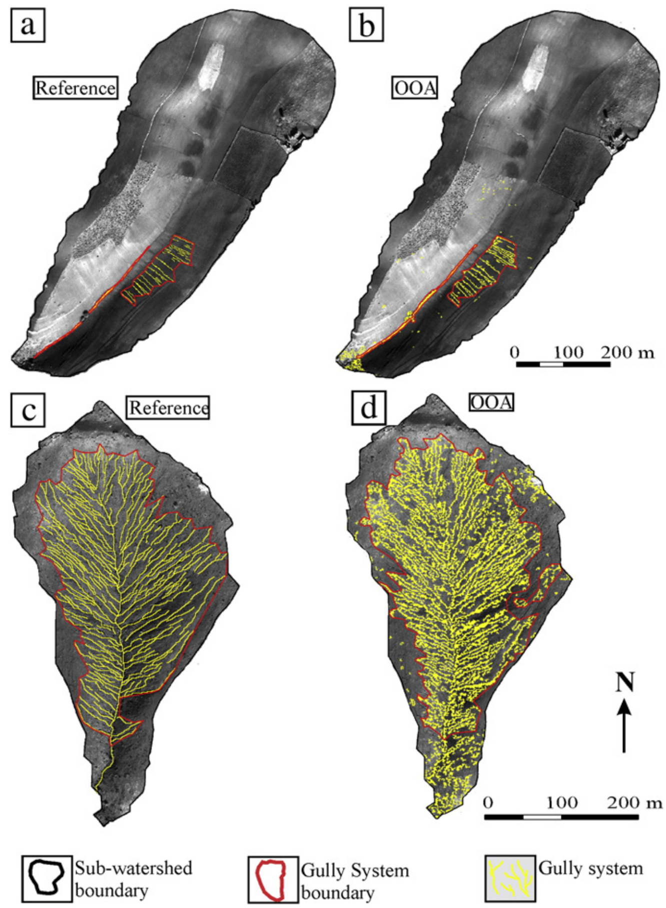

Fig. 9. Gully systems of reference (digitization by visual image interpretation) and OOA data (output from the rule-set developed) for two different sub-watersheds. (a and b) Simple and continuous gully system. (c and d) More complex and discontinuous gully system.

detecting gully erosion features, and is advanced compared to the existing methods. The time needed to map gullies for the entire test image (Fig. 7) was much shorter than the time to digitize gullies manually.

The use of OOA to map gullies was based only on the thresholds of physical parameters (slope, *SCA*, and *NDVI*) and information derived from satellite images (texture, contrast, and edge). The method is generic and the test for its transferability was also successful. Finer gully-related edges within the complex gully systems were better identified semi-automatically than by manual digitization which is subjective and dependent on individual visual acuity.

The potential users of the approach presented here are land managers interested in the location of gullies, the degree of land degradation, and gully dynamics over a period of time for the planning and implementation of soil conservation measures. The approach is also useful for the erosion research community, and can be further extended to provide more information such as gully dimensions and temporal changes of individual gullies.

Table 2
Difference in gully system area between that of the reference area (A_{REF}) and that from the OOA analysis (A_{OOA}).

Watershed	Watershed area, m^2	A_{REF}, m^2	A_{OOA}, m^2	Difference in area, m^2	% A_{REF}	% A_{OOA}	Over estimation
sw11	284,391	54,057	54,142	85	19.01	19.04	0.03
sw12	86,183	9956	11,485	1529	11.55	13.33	1.77

However, the following limitations of the approach were identified: (i) the thresholds used were subjective and require adaptation when the rule-set is used for a different region or imagery; (ii) the removal of false positives also remains empirical, and (iii) there is still room for better using process knowledge for gully formation. We will improve our gully detection method, and the results will be available on our website (www.itc.nl/OOA-group).

Acknowledgement

We wish to thank the DESIRE project for providing funds for conducting this study, and to the Geoeye foundation for the IKONOS imagery grant. We also thank Prof. Laouina Abdellah and his team, UNESCO-GN Chair, Unv. Mohammed V-Agdal, Rabat, for providing logistical support during the field work. Thanks to Andre Stumpf for assisting in conceptualization of texture measures based on the flow direction model. Thanks to the reviewers for their valuable comments.

References

Baatz, M., Schäpe, A., 2000. Multiresolution segmentation—an optimization approach for high quality multi-scale image segmentation. Angewandte Geographische Informationsverarbeitung XII. Herbert Wichmann Verlag, Karlsruhe, Germany, pp. 12–23.
Blaschke, T., 2010. Object based image analysis for remote sensing. ISPRS Journal of Photogrammetry and Remote Sensing 65, 2–16.
Bocco, G., Valenzuela, C.R., 1993. Integrating satellite remote sensing and Geographic Information Systems technologies in gully erosion research. Remote Sensing Reviews 7, 233–240.
Bocco, G., Palacio, J.L., Valenzuela, C.R., 1991. Gully erosion modeling using GIS and geomorphological knowledge. ITC Journal 3, 253–261.
Böhner, J., McCloy, K.R., Strobl, J. (Eds.), 2006. SAGA — Analyses and Modelling Applications: Göttinger Geographische Abhandlungen, 115.
Brooks, A.P., Shellberg, J.G., Knight, J., Spencer, J., 2009. Alluvial gully erosion: an example from the Mitchell fluvial megafan, Queensland, Australia. Earth Surface Processes and Landforms 34, 1951–1969.
Chen, Y.H., Su, W., Li, J., 2009. Hierarchical object oriented classification using very high resolution imagery and LIDAR data over urban areas. Advances in Space Research 43, 1101–1110.
De Asis, A.M., Omasa, K., Oki, K., Shimizu, Y., 2008. Accuracy and applicability of linear spectral unmixing in delineating potential erosion areas in tropical watersheds. International Journal of Remote Sensing 29, 4151–4171.
DESIRE, 2010. Study site description: Marmora, Morocco. http://www.desire-his.eu/wimba/CG%20SSD%20Marmora,%20Morocco/page_02.htm2010.
Dragut, L., Blaschkeb, T., 2006. Automated classification of landform elements using object-based image analysis. Geomorphology 81, 330–344.
Dragut, L., Tiede, D., Levick, R.S., 2010. ESP: a tool to estimate scale parameter for multiresolution image segmentation of remotely sensed data. International Journal of Geographical Information Science 24, 859–871.
Eustace, A., Matthew, P., Christian, W., 2009. Give me the dirt: detection of gully extent and volume using high-resolution LiDAR. In: Jones, S., Reinke, K. (Eds.), Innovations in Remote Sensing and Photogrammetry. Springer-Verlag, Berlin Heidelberg, pp. 255–269.
Greenlee, D.D., 1987. Raster and vector processing for scanned linework. Photogrammetric Engineering and Remote Sensing 53, 1383–1387.
Haralick, R.M., Shanmugam, K., Dinstein, I.H., 1973. Textural features for image classification. IEEE Transactions on Systems, Man and Cybernetics 3, 610–621.
Knight, J., Spencer, J., Brooks, A., Phinn, S., 2007. Large-area, high-resolution remote sensing based mapping of alluvial gully erosion in Australia's tropical rivers. Proceedings of the 5th Australian Stream Management Conference: Australian Rivers: Making a Difference. Charles Sturt University, Thurgoona, New South Wales, pp. 199–204.
Laliberte, A.S., Rango, A., 2009. Texture and scale in object-based analysis of subdecimeter resolution unmanned aerial vehicle (UAV) imagery. IEEE Transactions on Geoscience and Remote Sensing 47, 1–10.
Langran, K.J., 1983. Potential for monitoring soil erosion features and soil erosion modelling components from remotely sensed data. Proceedings of IGARSS'83, 31 August–2 September, San Francisco, California, pp. 2.1–2.4.
Lillesand, T.M., Kiefer, R.W., Chipman, J.W., 2008. Remote Sensing and Image Interpretation. Wiley & Sons, New York.
Martha, T.R., Kerle, N., Jetten, V.G., van Westen, C.J., Kumar, V., 2010a. Landslide volumetric analysis using Cartosat-1-derived DEMs. IEEE Geoscience and Remote Sensing Letters 7, 582–586.
Martha, T.R., Kerle, N., Jetten, V., van Westen, C.J., Kumar, K.V., 2010b. Characterising spectral, spatial and morphometric properties of landslides for semi-automatic detection using object-oriented methods. Geomorphology 116, 24–36.
Martha, T.R., Kerle, N., Jetten, V.G., van Westen, C.J., Kumar, V., in press. Segment optimisation and data-driven thresholding for knowledge-based landslide detection by object-oriented image analysis. IEEE Transaction on Geoscience and Remote Sensing.

Marzolff, I., Ries, J.B., 2007. Gully erosion monitoring in semi-arid landscapes. Zeitschrift für Geomorphologie 51, 405–425.
Melkman, A., 1987. On-line construction of the convex hull of a simple polygon. Information Processing Letters 25, 11–12.
Metternicht, G.I., Zinck, J.A., 1998. Evaluating the information content of JERS-1 SAR and Landsat TM data for discrimination of soil erosion features. ISPRS Journal of Photogrammetry & Remote Sensing 53, 143–153.
Perroy, R.L., Bookhagen, B., Asner, G.P., Chadwick, O.A., 2010. Comparison of gully erosion estimates using airborne and ground-based LiDAR on Santa Cruz Island, California. Geomorphology 118, 288–300.
Poesen, J., Nachtergaele, J., Verstraeten, G., Valentin, C., 2003. Gully erosion and environmental change: importance and research needs. Catena 50, 91–133.
Poesen, J., Vanwalleghem, T., Vent, J.D., Knapen, A., Verstraeten, G., Martinez-Casasnovas, A.J., 2006. Gully erosion in Europe. In: Boardman, J., Poesen, J. (Eds.), Soil Erosion in Europe. John Wiley & Sons Ltd, Chichester, pp. 515–536.
Seeger, M., Marzolff, I., Ries, J.B., 2009. Identification of gully-development processes in semi-arid NE-Spain. Zeitschrift für Geomorphologie 53, 417–431.
Shi, W.Z., Li, Q.Q., Zhus, C.Q., 2005. Estimating the propagation error of DEM from higher-order interpolation algorithms. International Journal of Remote Sensing 26, 3069–3084.
Singh, B.M., 1977. Interpretation of satellite imagery for delineation of ravines. Journal of Indian Society of Remote Sensing 1, 31–34.
Smith, H.T.U., 1943. Aerial Photographs and Their Application. Appleton Century Crofts, New York.
Stromquist, L.B., Lunden, Chakela, Q., 1985. Sediment sources, sediment transfer in a small Lesotho catchment: a pilot study of the spatial distribution of erosion features and their variation with time and climate. South African Journal of Geology 67, 3–13.
Stumpf, A., Kerle, N., in press. Object-oriented mapping of landslides using random forests. Remote Sensing of Environment.
Tansey, K., Chambers, I., Anstee, A., 2009. Object-oriented classification of very high resolution airborne imagery for the extraction of hedgerows and field margin cover in agricultural areas. Applied Geography 29, 145–157.
UNEP, 1994. United Nations Environmental Programme. United Nations Conventions to Combat Desertification in Those Countries Experiencing Serious Drought and/or Desertification, Particularly in Africa, Geneva, Switzerland.
Valentin, C., Poesen, J., Li, Y., 2005. Gully erosion: impacts, factors and control. Catena 63, 132–153.
van Dijck, S.J.E., Laouina, A., Carvalho, A.V., Loos, S., Schipper, A.M., Van der Kwast, H., Nafaa, R., Antari, M., Rocha, A., Borrego, C., Ritsema, C.J., 2006. Desertification in northern Morocco due to effects of climate change on groundwater recharge. In: Kepner, W.G., Rubio, J.L., Mouat, D.A., Fausto, P. (Eds.), Desertification in the Mediterranean Region: A Security Issue. Springer, Dordrecht, pp. 549–577.
Vrieling, A., Rodrigues, S.C., 2004. Erosion Assessment in the Brazilian Cerrados Using Multi-Temporal SAR Imagery. Proceedings of the 2004 Envisat and ERS Symposium, Salzburg, Austria.
Vrieling, A., Rodrigues, S.C., Bartholomeus, H., Sterk, G., 2007. Automatic identification of erosion gullies with ASTER imagery in the Brazilian Cerrados. International Journal of Remote Sensing 28, 2723–2738.
Zhang, L., Gruen, A., 2006. Multi-image matching for DSM generation from IKONOS imagery. ISPRS Journal of Photogrammetry and Remote Sensing 60, 195–211.